



**HAL**  
open science

## The role of Mie scattering in the seeding of matter-wave superradiance

Romain Bachelard, Helmar Bender, Philippe W. Courteille, Nicola Piovella,  
Christian Stehle, Claus Zimmermann, Sebastian Slama

► **To cite this version:**

Romain Bachelard, Helmar Bender, Philippe W. Courteille, Nicola Piovella, Christian Stehle, et al..  
The role of Mie scattering in the seeding of matter-wave superradiance. 2012. hal-00702284v2

**HAL Id: hal-00702284**

**<https://hal.science/hal-00702284v2>**

Preprint submitted on 26 Jul 2012 (v2), last revised 19 Sep 2012 (v3)

**HAL** is a multi-disciplinary open access archive for the deposit and dissemination of scientific research documents, whether they are published or not. The documents may come from teaching and research institutions in France or abroad, or from public or private research centers.

L'archive ouverte pluridisciplinaire **HAL**, est destinée au dépôt et à la diffusion de documents scientifiques de niveau recherche, publiés ou non, émanant des établissements d'enseignement et de recherche français ou étrangers, des laboratoires publics ou privés.

# The role of Mie scattering in the seeding of matter-wave superradiance

R. Bachelard<sup>a</sup>, H. Bender<sup>a,c</sup>, and Ph.W. Courteille<sup>a</sup>

<sup>a</sup>*Instituto de Física de São Carlos, Universidade de São Paulo, 13560-970 São Carlos, SP, Brazil*

N. Piovella<sup>b</sup>

<sup>b</sup>*Dipartimento di Fisica, Università Degli Studi di Milano and INFN, Via Celoria 16, I-20133 Milano, Italy*

C. Stehle<sup>c</sup>, C. Zimmermann<sup>c</sup>, and S. Slama<sup>c</sup>

<sup>c</sup>*Physikalisches Institut, Eberhardt-Karls-Universität Tübingen, D-72076 Tübingen, Germany*

(Dated: July 26, 2012)

Matter-wave superradiance is based on the interplay between ultracold atoms coherently organized in momentum space and a backscattered wave. Here, we show that this mechanism may be triggered by Mie scattering from the atomic cloud. We show how the laser light populates the modes of the cloud, and thus imprints a phase gradient on the excited atomic dipoles. The interference with the atoms in the ground state results in a grating, that in turn generates coherent emission, contributing to the backward light wave onset. The atomic recoil 'halos' created by the scattered light exhibit a strong anisotropy, in contrast to single-atom scattering.

PACS numbers: 42.50.Ct, 03.75.-b, 42.50.Gy

Matter wave superradiance (MWSR) [1] and collective atomic recoil lasing (CARL) [2, 3] are light-induced instabilities of the density distribution in atomic clouds. More precisely, they are due to correlations between successive scattering events mediated by long-lived coherences in the motional state of an (ultracold) atomic cloud or in the light field of an optical resonator [4]. Despite considerable theoretical efforts having been devoted to the dynamics of MWSR [5–7], open questions still remain. One of them concerns the seeding mechanism which is able to start the MWSR instability also in the presence of losses. Thermal and quantum fluctuations will naturally give contributions, however, in this paper we point out the particular role of Mie scattering which turns out to be important at the onset of MWSR. Being active before any instability has developed, it induces a *phase* correlation between the atomic dipoles which favors the build up of an instability.

The below-threshold dynamics and the seeding of matter-wave superradiance are interesting problems. As long as we consider the atomic cloud as a homogeneous entity, e.g. a Bose-Einstein condensate (BEC) in the mean field description, no scattering should occur at all. Theoretical models which describe BECs as matter waves without fluctuations thus fail to explain how MWSR starts when no seeding wave is present [8]. On the other hand, recent work has shown [9, 10] how atomic coarse-graining, density fluctuations and Mie scattering from finite-sized clouds can influence the scattering even of a single photon. Also optical cavities may strongly affect the scattering by shaping the angular distribution of the density of modes that are capable of receiving the scattered photons [11]. These processes have a decisive impact on the mode competition preceding the exponential instability, and hence on the instability itself.

Here we show, that Mie scattering, caused by the finite size of the atomic cloud, favors the formation of a matter wave dipole grating. This has already been suspected in [12]. Indeed, prior to any significant motion of the atoms, their dipoles collectively order which in turn leads to coherent emission.

In previous papers [13–16], we discussed the impact of atomic coarse-graining and finite scattering volumes on the radiation pressure force which acts on the cloud's center-of-mass. Here, we investigate the momentum distribution after the cooperative scattering of the laser light by a BEC. Our theoretical model describes the atomic cloud as a macroscopic matter wave which is homogeneously distributed within a sphere, i.e. the atoms are considered to be strongly delocalized and density fluctuations are neglected. We find that the momentum distribution of the atoms adopts the shape of a **recoil halo**, very similar to the ones observed experimentally in time-of-flight images of BECs. The halo indicates the directions into which the atoms are preferentially scattered **before** the density distribution is noticeably modified. In particular, it exhibits a pronounced peak at  $2\hbar k$ . This corresponds to an increased backscattering of light, that acts as a seed for MWSR.

We consider an homogeneous spherical cloud of two-level atoms shined by a laser of wavevector  $\mathbf{k}_0 = k_0 \hat{z}$ , Rabi frequency  $\Omega_0$  and detuned from the atomic transition by  $\Delta_0$ . The atomic cloud is described as a bosonic ensemble of  $N$  two-level atoms with field operator  $\hat{\Psi}(\mathbf{r}, t) = \hat{\Psi}_g(\mathbf{r}, t) + \hat{\Psi}_e(\mathbf{r}, t)$  ( $g$  for the ground state,  $e$  for the excited one). We treat the condensate as an ideal gas and consider the scattering between matter wave and optical waves, but neglect nonlinearities due to atom-atom interaction. In second quantization, the interaction between the atoms and light is described by the Hamil-

tonian [13, 17]

$$\hat{H}(t) = \frac{\hbar\Omega_0}{2} \int d\mathbf{r} \left[ \hat{\Psi}_e^\dagger(\mathbf{r}, t) \hat{\Psi}_g(\mathbf{r}, t) e^{-i\Delta_0 t + i\mathbf{k}_0 \cdot \mathbf{r}} + h.c. \right] \quad (1)$$

$$+ \hbar \sum_{\mathbf{k}} g_{\mathbf{k}} \int d\mathbf{r} \left[ \hat{\Psi}_e^\dagger(\mathbf{r}, t) \hat{\Psi}_g(\mathbf{r}, t) \hat{a}_{\mathbf{k}} e^{-i\Delta_k t + i\mathbf{k} \cdot \mathbf{r}} + h.c. \right],$$

where the first (second) line describes the absorption and emission of a pump mode  $\Omega_0$  (a vacuum mode  $\hat{a}_{\mathbf{k}}$ ). Doppler effects are neglected. Replacing  $\hat{\Psi}_e(\mathbf{r}, t) \rightarrow \hat{\Psi}_e(\mathbf{r}, t) e^{i\Delta_0 t}$  induces an energy shift of  $-\Delta_0 |\hat{\Psi}_e|^2$  in the Hamiltonian from which the Heisenberg equations may be derived:

$$\frac{\partial \hat{\Psi}_g}{\partial t} = -i\hat{\Psi}_e \left[ \frac{\Omega_0}{2} e^{-i\mathbf{k}_0 \cdot \mathbf{r}} + \sum_{\mathbf{k}} g_{\mathbf{k}} \hat{a}_{\mathbf{k}}^\dagger e^{-i(\Delta_0 - \Delta_k)t - i\mathbf{k} \cdot \mathbf{r}} \right] \quad (2)$$

$$\frac{\partial \hat{\Psi}_e}{\partial t} = -i\hat{\Psi}_g \left[ \frac{\Omega_0}{2} e^{i\mathbf{k}_0 \cdot \mathbf{r}} + \sum_{\mathbf{k}} g_{\mathbf{k}} \hat{a}_{\mathbf{k}} e^{i(\Delta_0 - \Delta_k)t + i\mathbf{k} \cdot \mathbf{r}} \right]$$

$$+ i\Delta_0 \hat{\Psi}_e \quad (3)$$

$$\frac{d\hat{a}_{\mathbf{k}}}{dt} = -ig_{\mathbf{k}} e^{-i(\Delta_0 - \Delta_k)t} \int d\mathbf{r} \hat{\Psi}_g^\dagger(\mathbf{r}, t) \hat{\Psi}_e(\mathbf{r}, t) e^{-i\mathbf{k} \cdot \mathbf{r}}. \quad (4)$$

For large atom numbers and for far detuning from the atomic transition frequency, one can neglect quantum fluctuations and treat the operators as c-numbers ( $\hat{\Psi} \rightarrow \psi$ ,  $\hat{a}_{\mathbf{k}} \rightarrow a_{\mathbf{k}}$ ). Eq.(4) is integrated over time as

$$a_{\mathbf{k}} = -ig_{\mathbf{k}} \int_0^t dt' e^{-i(\Delta_0 - \Delta_k)t'} \int d\mathbf{r} \psi_g^*(\mathbf{r}, t') \psi_e'(\mathbf{r}, t) e^{-i\mathbf{k} \cdot \mathbf{r}}, \quad (5)$$

and inserted into (3). Furthermore, we switch to a continuous-mode description  $\sum_{\mathbf{k}} \rightarrow (V_\nu / (2\pi)^3) \int d\mathbf{k}$  and obtain:

$$\frac{\partial \psi_e}{\partial t} = i\Delta_0 \psi_e(\mathbf{r}, t) - i\frac{\Omega_0}{2} e^{i\mathbf{k}_0 \cdot \mathbf{r}} \psi_g(\mathbf{r}, t) - \psi_g(\mathbf{r}, t) \int d\mathbf{r}' \quad (6)$$

$$\times \int d\mathbf{k} g_{\mathbf{k}}^2 e^{i\mathbf{k} \cdot (\mathbf{r} - \mathbf{r}')} \int_0^t dt' e^{i(\Delta_0 - \Delta_k)(t-t')} \psi_g^*(\mathbf{r}', t') \psi_e(\mathbf{r}', t').$$

We consider time scales over which the atomic density does not significantly change, i.e.  $\psi_g(\mathbf{r}, t) \approx \psi_{g0}(\mathbf{r})$  in (6), with  $\rho_0(\mathbf{r}) = |\psi_{g0}(\mathbf{r})|^2$  being the initial density of the cloud. Using the Markov approximation, i.e. the photon time of flight through the cloud is much shorter than the atomic decay time, the last integral in (6) is replaced by  $\delta(k - k_0) \psi_{g0}(\mathbf{r}') \psi_e(\mathbf{r}', t) / c$ . With the assumption that all the electromagnetic modes are equally present in the system ( $g_{\mathbf{k}} \approx g_{k_0}$ ) and by keeping rotating-wave-approximation terms, one can show that [18]:

$$\int d\mathbf{k} g_{\mathbf{k}}^2 e^{i\mathbf{k} \cdot \mathbf{d}} \int_0^\infty dt' e^{i(\Delta_0 - \Delta_k)(t-t')} = \frac{\Gamma}{2ik_0|\mathbf{d}|} e^{ik_0|\mathbf{d}|}, \quad (7)$$

where  $\Gamma = V_\nu g_{k_0}^2 k_0^2 / \pi c$  is the atomic decay rate. For the normalized excitation field  $\beta(\mathbf{r}, t) = \psi_e(\mathbf{r}, t) / \psi_{g0}(\mathbf{r})$  with

$|\beta(\mathbf{r})|^2$  being the probability for an atom to be excited, one obtains [27]

$$\frac{\partial \beta(\mathbf{r}, t)}{\partial t} = \left( i\Delta_0 - \frac{\Gamma}{2} \right) \beta(\mathbf{r}, t) - i\frac{\Omega_0}{2} e^{i\mathbf{k}_0 \cdot \mathbf{r}}$$

$$- \frac{\Gamma}{2} \int d\mathbf{r}' \rho_0(\mathbf{r}') \frac{\exp(i\mathbf{k}_0 \cdot |\mathbf{r} - \mathbf{r}'|)}{ik_0|\mathbf{r} - \mathbf{r}'|} \beta(\mathbf{r}', t). \quad (8)$$

which recovers the model of cooperative scattering of a plane-wave introduced in [13].

Eq.(8) can be used to describe the scattering of light from a dielectric medium with an index of refraction  $m_c = \sqrt{1 - 4\pi\rho_0\Gamma/k_0^3(\Delta_0 + i\Gamma/2)}$  in the steady-state regime [16]. The excitation pattern inside the cloud can be calculated analogous to Mie's theory [19, 20]: the electromagnetic fields inside and outside the cloud are decomposed into modes, thereafter labeled  $n$ , that are elementary solutions of the Helmholtz equation  $(\Delta + m_c^2 k_0^2)\beta = 0$ . Their amplitudes  $\beta_n$  are calculated according to the continuity conditions of the fields at the edge of the sphere. For a homogeneous spherical cloud of radius  $R$ , the field  $\beta(\mathbf{r})$  reads:

$$\beta(\mathbf{r}) = \frac{dE_0}{\hbar\Gamma} \sum_{n=0}^{\infty} (2n+1) i^n \beta_n j_n(m_c k_0 r) P_n(\cos\theta), \quad (9)$$

with  $j_n$  the spherical Bessel functions and  $P_n$  the Legendre polynomials (see e.g. [16] for an expression of the scattering coefficients  $\beta_n$ ). Thus, the laser imprints a phase, with wavevector  $m_c k_0$ , to the excited state  $\psi_e$ , which interferes with the ground state  $\psi_g$  which has a constant phase. The resulting grating is at the origin of coherent emission and of the backscattering wave that acts as a seed for MWSR. Indeed, the field radiated by the atoms inside the cloud in a direction  $\mathbf{u}(\theta, \phi)$  is proportional to the structure factor:

$$s_c(\mathbf{u}) = \frac{1}{N} \int \rho(\mathbf{r}) \beta(\mathbf{r}) e^{-im_c k_0 \mathbf{u} \cdot \mathbf{r}} d\mathbf{r}, \quad (10)$$

with the index of refraction  $m_c$  given above. Hence, the coherent emission by the cloud is a direct consequence of periodic excitation field and the resulting grating.

The scattered light is difficult to observe directly, however, the radiation pattern is also present in the momentum distribution of the atoms which can be easily recorded by time of flight imaging. Different to an  $N$ -body model, the quantum matter field approach yields the momentum distribution simply as the Fourier transform of the matter field,  $\hat{\psi}(\mathbf{p}) = (2\pi\hbar)^{-3} \int \psi(\mathbf{r}) e^{-i\mathbf{p} \cdot \mathbf{r} / \hbar} d\mathbf{r}$ . Hence, for an homogeneous cloud, the momentum distribution of the excited state is directly proportional to the structure factor:  $\hat{\psi}_e(\mathbf{p}) \propto s_c(\mathbf{p}/\hbar)$ , with  $\mathbf{p} = m_c \hbar \mathbf{k}$  and  $\mathbf{k} = k_0 \mathbf{u}$ . Using Eq.(9), it can be deduced that the momentum wavefunction  $\hat{\psi}_e$  for an uniform sphere of radius  $R$  reads:

$$\hat{\psi}_e(\mathbf{p}) = \frac{dE_0 \sqrt{\rho_0}}{\hbar\Gamma(2\pi\hbar)^3} \sum_{n=0}^{\infty} (2n+1) \beta_n \gamma_n(p) P_n(\cos\theta), \quad (11)$$

with  $\gamma_n(p) = 4\pi \int_0^R r^2 j_n(m_c k_0 r) j_n(pr/\hbar) dr$ . For a very

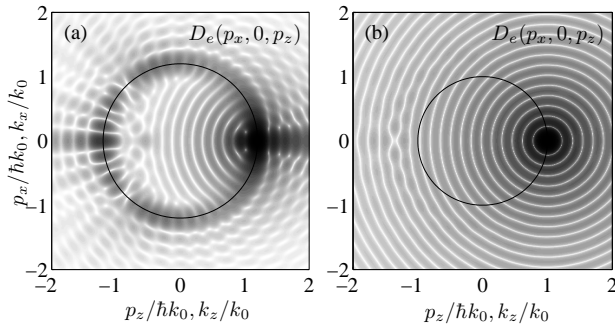


FIG. 1. Momentum distribution of the excited state  $D_e = |\hat{\psi}_e|^2$ , in logarithmic scale. The emission pattern  $|s_c(\mathbf{k})|^2$  concentrates around a circle with radius  $p = m_c \hbar k_0$  (black line). Simulations for a laser detuning  $\Delta_0 = -3\text{GHz}$  and a cloud (a) of size  $k_0 R = 20$ , atom number  $N = 1.15 \times 10^6$  and refractive index  $m_c = 1.2$ , (b) of size  $k_0 R = 20$ , atom number  $N = 100$  and refractive index  $m_c = 1 + 2.10^{-7}$  ( $\Delta_0 = -488\text{MHz}$ ). For rubidium,  $k_0^{Rb} = 8.05 \times 10^6 \text{m}^{-1}$  and  $\Gamma^{Rb} = 6.1\text{MHz}$ .

small cloud ( $k_0 R \ll 1$ ), as expected from Rayleigh theory, the scattering of light is isotropic since only the first Mie mode ( $n = 0$ ) is populated. However, for large many-particle spheres, Mie scattering turns out to be fundamentally anisotropic, as many modes are populated. Fig.1(a) shows a typical momentum distribution of the excited atoms  $|\hat{\psi}_e(\mathbf{p})|^2$  and the associated scattering pattern  $|s_c(\mathbf{k})|^2$  of the light. Although most atoms recoil to  $\mathbf{k} = k_0 \hat{z}$ , a significant amount of light is scattered backward ( $\mathbf{k} = -k_0 \hat{z}$ ) and acts as a seed for the MWSR instability.

Note that the momentum distribution  $D_e(\mathbf{p}) = |\hat{\psi}_e(\mathbf{p})|^2$  is concentrated along a circle with radius  $p = m_c \hbar k_0$  rather than  $\hbar k_0$  (i.e. that  $\gamma_n(p)$  reaches a maximum for  $p = m_c \hbar k_0$ ). This is a signature of the Minkowski momentum for atomic recoil, that characterizes the momentum exchanged between light and matter in dielectric media [21]. The blurring of the momentum wavefunction along the circle originates in the finite size of the cloud, that creates a natural momentum spread  $\sigma_p \sim \hbar/R$ . The ripples of the distribution are due to the sharp boundary of the cloud's density, yielding a Fourier transform with many secondary peaks.

On the other hand, in optical dilute clouds, almost all the light is scattered forward, leaving the incoming light almost untouched. Such a scattering pattern is displayed in Fig.1(b), where the intricate pattern of Mie scattering by optically dense cloud has disappeared. In this limit, the excitation field is often approximated by the timed Dicke state  $\beta(\mathbf{r}) \sim \beta_{TDS} e^{i\mathbf{k}_0 \cdot \mathbf{r}}$  [22], yet such an ansatz fails to predict any three-dimensional recoil pattern.

After an atom absorbs a photon from the laser with a momentum kick  $m_c \hbar k_0$ , the photon is reemitted according to the Mie pattern  $s_c(\mathbf{p}/\hbar) \propto \hat{\psi}_e(\mathbf{p})$ . Thus the atom

will gain an extra momentum  $m_c \hbar k_0$  with a direction opposite to the emitted photon and the momentum pattern of the ground state atoms after the scattering process is given by  $|\hat{\psi}_e(m_c \hbar \mathbf{k}_0 - \mathbf{p})|^2$ . Experimentally, the column-integrated momentum distribution is observed in time of flight images. This leads to defining the projected distribution  $D_g^y(p_x, p_z) = \int |\hat{\psi}_g(\mathbf{p})|^2 dp_y$ . Such an integrated distribution is presented in Fig.2(a). The atoms are observed to *inhomogeneously* fill a circle of radius  $m_c \hbar k_0$ . In particular, the part of the sphere around  $\mathbf{p} = (3/2)\hbar \mathbf{k}_0$  is weakly populated, which reflects the anisotropic nature of Mie scattering.

Experimentally, the atomic recoil patterns are investigated by using the set-up of [10]. After the interaction with the light, the  $^{87}\text{Rb}$  atoms ballistically expand for  $t_F = 20\text{ms}$ . The density distribution of the expanded cloud is recorded by standard absorption imaging yielding the initial momentum distribution before the expansion according to  $\mathbf{p} = m_{Rb} \mathbf{r}/t_F$  (the initial size of the cloud  $\sim 20\mu\text{m}$  is much smaller than its expanded size at the time of imaging).

The integrated momentum distribution observed experimentally reproduces the features predicted by Mie scattering (see Fig.2(b)). A sphere of radius  $\hbar k_0$  is filled with atoms, yet it exhibits a region where the probability of the atomic recoil is very low around  $p_z = 1.5\hbar k_0$ . Moreover, it can be observed that a large number of atoms recoil around the  $\mathbf{p} = 2\hbar \mathbf{k}_0$ , that are the signature of the backward emitted wave. The presence of preferred directions of emission is associated to the presence of Mie resonances [16], and the increase of emission in these directions can be interpreted as a self Purcell enhancement [23] since the cloud acts as a cavity on himself to modify its emission. This is opposite to single-atom scattering that scatter light in random directions, and not particularly backward and forward.

It is important to note that Mie scattering is a three-dimensional process, while the MWSR only develops along its most unstable direction. Mie scattering is a seeding process that sends light in many directions, particularly also backwards, which is known to be the most unstable direction for MWSR in a cigar-shaped cloud illuminated along its main axis [24].

These two processes are illustrated in Fig.3. Initially, Mie scattering populates a sphere of radius  $p \approx m_c \hbar k_0$ . Then a MWSR instability develops, i.e. the grating induces light emission that, in turn, starts amplifying this atomic grating. The atoms observed in  $\mathbf{p} \approx -2m_c \hbar \mathbf{k}_0$  and  $\mathbf{p} \approx 4m_c \hbar \mathbf{k}_0$  are not predicted by Mie scattering and can be explained only by the self-consistent matter-wave dynamics.

In this paper we showed that Mie scattering induces a grating in the atomic distribution even below the threshold for the MWSR instability. Its signature is an anisotropic three-dimensional halo in the atomic momentum distribution. The atoms observed at  $\mathbf{p} \approx 2\hbar \mathbf{k}_0$  gen-

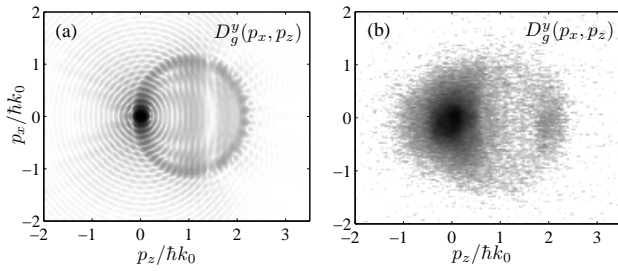


FIG. 2. (a) Integrated momentum distribution of the ground state, calculated from Eq.11 for a spherical homogeneous cloud of radius  $k_0 R = 29.6$ ,  $\Delta_0 = -15\text{GHz}$  and with a refractive index  $m_c = 1.067$  (a low-pass Gaussian filter was applied to attenuate the ripples due to the sharp boundaries of the homogeneous clouds, since they are irrelevant for comparison with the experiment) (b) Experimental integrated momentum distribution of the ground state for an ellipsoidal cloud of length  $k_0 \sigma_z \sim 29.6$ , transverse radius  $k_0 \sigma_\perp \sim 4.7$ , with  $N \sim 147000$  atoms and a laser detuning  $\Delta_0 = -15\text{GHz}$  and a  $20\mu\text{s}$  laser pulse of  $17\text{mW}$ . Its refractive index is  $m_c \approx 1.067$ .

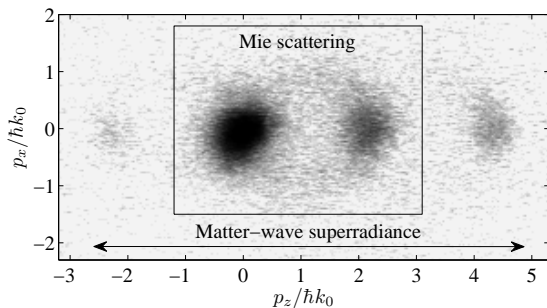


FIG. 3. Momentum distribution  $|\hat{\psi}_g|^2$  above the threshold of the MWSR. Experiment realized with an ellipsoidal cloud of transverse radius  $k_0 \sigma_\perp \sim 3.5$ , length  $k_0 \sigma_z \sim 22$ , with  $N \sim 156000$  atoms and a laser detuning  $\Delta_0 = -15\text{GHz}$ .

erate a seeding wave for MWSR. Indeed, the matter wave modes at  $0$  and  $2\hbar\mathbf{k}_0$  together form density grating at which subsequent light injected from the pump laser are Bragg-scattered in a self-amplifying process.

Remark that quantum fluctuations and disorder may also give rise to backward emission [25], and thus act as a seed for the matter-wave superradiance. These effects will be included in an extended work.

Finally, it is interesting to remark that the off-axis emission of photons should be associated to higher modes ( $n \gg 1$ ) that correspond to photons with long lifetime within the cloud [26]. Thus, a time-resolved observation of the off-axis atomic recoils should bear the signature of subradiance.

We acknowledge helpful discussion with R. Kaiser. This work has been supported by the Fundação de Am-

paro Pesquisa do Estado de São Paulo (FAPESP) and the Research Executive Agency (program COSCALI, No. PIRSES-GA-2010- 268717). C.S., C.Z and S.S acknowledge support by the Deutsche Forschungsgemeinschaft.

- 
- [1] S. Inouye, *et al.*, Science **285**, 571 (1999).
  - [2] R. Bonifacio and L. De Salvo, Nucl. Instrum. Methods A **341**, 360 (1994).
  - [3] D. Kruse, Ch. von Cube, C. Zimmermann, and Ph.W. Courteille, Phys. Rev. Lett. **91**, 183601 (2003).
  - [4] S. Slama *et al.*, Phys. Rev. Lett. **98**, 053603 (2007).
  - [5] N. Piovella, R. Bonifacio, B.W.J. McNeil, and G.R.M. Robb, Opt. Commun. **187**, 165 (1997).
  - [6] N. Piovella, M. Gatelli, and R. Bonifacio, Opt. Commun. **194**, 167 (2001).
  - [7] W. Ketterle and Shin Inouye, C. R. Acad. Sci., Ser. IIB **2**, 339 (2001) and cond-mat/0101424.
  - [8] M. Kozuma *et al.*, Science **286**, 2309 (1999).
  - [9] T. Bienaimé, *et al.*, Phys. Rev. Lett. **104**, 183602 (2010).
  - [10] H. Bender, *et al.*, Phys. Rev. A **82**, 011404(R) (2010).
  - [11] S. Bux, Ch. Gnahn, R.A. Maier, C. Zimmermann, Ph.W. Courteille, Phys. Rev. Lett. **106**, 203601 (2011).
  - [12] W. Ketterle, Phys. Rev. Lett. **106**, 118901 (2010).
  - [13] Ph.W. Courteille, S. Bux, E. Lucioni, K. Lauber, T. Bienaimé, R. Kaiser, and N. Piovella, Eur. Phys. J. D **58**, 69 (2010).
  - [14] S. Bux, *et al.*, J. Mod. Opt. **57**, 1841 (2010).
  - [15] R. Bachelard, N. Piovella, Ph.W. Courteille, Phys. Rev. A **84**, 013821 (2011).
  - [16] R. Bachelard, Ph.W. Courteille, R. Kaiser, N. Piovella, Europhys. Lett. **97**, 14004 (2012).
  - [17] T. Bienaimé, M. Petruzzo, D. Bigerni, N. Piovella, R. Kaiser, J. of Mod. Opt. **58**, 1942 (2011).
  - [18] A.A. Svidzinsky, J.-T. Chang, and M.O. Scully, Phys. Rev. A **81**, 053821 (2010).
  - [19] G. Mie, Ann. Phys. **330**, 377 (1908), "Beiträge zur Optik trüber Medien, speziell kolloidaler Metallösungen".
  - [20] C.F. Bohren and D.R. Huffman, *Absorption and Scattering of Light from Small Particles*, Wiley, (1998).
  - [21] G.K. Campbell, *et al.*, Phys. Rev. Lett. **94**, 170403 (2005).
  - [22] M.O. Scully, E.S. Fry, C.H. Raymond Ooi, and K. Wdkiewicz, Phys. Rev. Lett. **96**, 010501 (2006).
  - [23] E. M. Purcell, Phys. Rev. **69**, 681 (1946).
  - [24] M. G. Moore and P. Meystre, Phys. Rev. Lett. **83**, 5202 (1999).
  - [25] D. Wilkowski *et al.*, J.O.S.A B **21**, 183 (2004).
  - [26] T. Bienaimé, N. Piovella and R. Kaiser, Phys. Rev. Lett. **108**, 123602 (2012).
  - [27] The single-atom spontaneous decay term  $-(\Gamma/2)\beta$  in Eq.(8) arises from the non-commutation properties of the bosonic operators  $\hat{\Psi}_g$  and  $\hat{\Psi}_e$ , analogously to the spontaneous emission from vacuum arising from the commutation rule for  $\hat{a}_{\mathbf{k}}$ . The single-atom decay term, however, is negligible far from the atomic transition ( $\Delta_0 \gg \Gamma$ ), as will be assumed in the present work.